Formation and Migration of Carbon Produced in the Dissociation of CO on Rh/TiO_2(110)−(1 × 2) Model Catalyst: A Scanning Tunneling Microscopy Study

A. Berkó, T. Bíró, and F. Solymosi*

Reaction Kinetics Research Group of the Hungarian Academy of Sciences and Department of Solid State and Radiochemistry, Attila József University, P.O. Box 168, H-6701, Szeged, Hungary

Received: July 20, 1999; In Final Form: January 4, 2000

Scanning tunneling microscopy (STM) completed by Auger-electron spectroscopy (AES) and thermal desorption spectroscopy (TDS) measurements was applied for investigating the formation and thermal-induced migration of carbon nanoclusters produced by the decomposition of CO on Rh/TiO_2(110)−(1 × 2) planar catalyst. The annealing of a clean TiO_2(110)−(1 × 2) surface in a CO atmosphere (few millibar pressure) at 500 K results in the reconstruction of the (1 × 2) structure into the (1 × 4) arrangement. The same treatment of an Rh/TiO_2(110)−(1 × 2) catalyst containing well-separated Rh nanocrystallites of approximately 10 nm in diameter leads to the formation of 3D carbon nanoclusters of 1−2 nm size. A fraction of the carbon formed on Rh nanoparticles diffuses (probably also in cluster form) onto the support already at 500 K (spillover). In the temperature range of 700−1100 K the carbon clusters agglomerate and collapse into larger nanoparticles. The accumulation of carbon on the existing Rh nanoparticles occurs at above 1100 K. Annealing at 1300 K causes the recovering of the original morphology of the Rh/TiO_2 (110)−(1 × 2) catalyst, suggesting a total gasification of the surface carbon. These processes are accompanied by the oxidation of surface carbon by the bulk oxygen of titania resulting in the formation of CO in the temperature range 800−1300 K.

Introduction

The carbon deposits formed in numerous surface reactions are considered as key intermediates in the hydrocarbon catalysis.[1] Recently, this interest has increased tremendously by the invention of the catalytic production of fullerene-like species.[2−15] In these works mainly hydrocarbons were used in the chemical vapor deposition (CVD) process as a carbon source; however, CO also proved to be a well-applicable feedstock, especially for growing single-wall nanotubes.[6−8] It has been demonstrated that there is a strong correlation between the diameter of the metal nanoparticles and that of the carbon nanotubes formed in the catalytic process.[2,5,6,8,12] This observation was explained by the nucleation of a carbon shell on the supported metal nanoparticles with subsequent formation of a fullerene tube.[6,11,15]

Concerning the interaction between CO and supported metal nanoparticles, it is well-known that the shape and integrity of the metal particles can be radically changed by CO adsorption, as was revealed first by EXAFS for Rh/Al_2O_3 and further studied by means of IR spectroscopy.[16−18] Similar features were observed for supported Ru, Ir, and Re.[19−23] Recently, the adsorption-induced structural changes of Rh and Ir nanoparticles were demonstrated by scanning tunneling microscopy (STM)[24−26] and SPA-low-energy electron diffraction (SPA-LEED).[27] It appeared that the effect of CO strongly depends on the size of the supported nanoparticles: a very rapid disintegration of Rh particles of the size 1−2 nm to atomically dispersed Rh was observed at 300 K. The CO-induced process became slower for larger particles with a size of 3−4 nm, and it did not occur at all for large Rh clusters (8−10 nm) even at higher (10 mbar) CO pressure. At higher temperatures, above 400 K, CO induced the opposite process, i.e., the agglomeration of Rh nanoparticles into larger ones.[24,26] In these investigations we noticed that the treatment of Rh/TiO_2 in CO at higher pressures (1−10 mbar) and at higher temperatures (>500 K)—when we can count with the dissociation/disproportionation of CO—results in the formation of new nanoparticles, probably carbon nanoclusters.

The dissociation and disproportionation of CO on supported Rh clusters were studied first in our laboratory.[28,29] As regards the effect of the nature of the supports, titania was found to be the most effective support, which was attributed to an electronic interaction between titania and Rh.[29] An interesting finding of this study was that the amount of carbon formed was much larger than the number of surface Rh atoms, which suggested that a fraction of carbon is located on the titania support. The occurrence of the dissociation of CO on Rh single-crystal surfaces under ultrahigh-vacuum (UHV) conditions has been the subject of extensive studies and debate.[30−38] The generally accepted conclusion from these works is that the dissociation of CO proceeds on stepped, defective, and more open (210) Rh surfaces but it does not occur on the flat close-packed (111) plane. Recently, a size dependence of CO dissociation on Rh islands deposited on a thin Al_2O_3 film was reported.[39,40]

The primary aim of this work is to follow the formation and thermal behavior of carbon clusters produced in the dissociation of CO on Rh/TiO_2(110)−(1 × 2) model catalyst by the STM method. We believe that the detailed knowledge of the low-temperature graphitization of transition metal particles may contribute to the elaboration of the controlled production of different types of fullerene nanotubes.

Experimental Section

The experiments were carried out in an UHV chamber equipped with quadrupole mass spectrometer, three-grid AES-LEED analyzer and commercial STM head (WA-Technology). The polished TiO_2(110) single-crystal sample was purchased

* Corresponding author. E-mail: Frigyes.Solymosi@chem.u-szeged.hu.

10.1021/jp9924981 CCC: $19.00
Published on Web 02/24/2000

from PI-KEM. The probe was clipped by a Ta plate on a transferable sample holder and heated by a W filament positioned just below the plate. By this arrangement it was possible to achieve temperatures as high as 1300 K, which was measured by a thin chromel−alumel thermocouple forced to the edge of the sample. The cleaning procedure of the probe was described in previous papers.[41,42] The annealing of the cleaned sample at 800−900 K resulted in a bulk-terminated 1×1 surface. Highly ordered 1×2 reconstructed terraces covering 80−90% of the total surface area could be obtained after extended annealing above 1100 K.

The evaporation of Rh was performed by ohmic heating of a high-purity Rh filament. During the dosing of admetal the distance between the evaporator and the TiO_2 sample was approximately 20 mm. The rate of deposition was controlled by adjusting the current flowing through the Rh filament spot-welded to a thicker Ta rod. The amount and cleanliness of the epitaxial Rh layer was monitored by AES spectroscopy. The surface concentration of the deposited metal is given in monolayer equivalent (ML), which corresponds to approximately 1.6×10^{15} atoms/cm^2. The determination of the amount of Rh was based on the calculation of the appearing volume of 3D Rh crystallites observed after annealing at 1200 K by STM. This method was applied and described in detail earlier.[41] High-purity CO (99.97%) gas was used in the experiments, and it was checked in the gas phase by quadrupole mass spectrometry and infrared absorption spectroscopy.

Results and Discussion

Preparation of Supported Rh Nanoparticles with a Large Interparticle Distance on the $TiO_2(110)-(1 \times 2)$ Surface. The preparation of metal nanoparticles and their characterization have been the subject of numerous recent studies. The results obtained are well documented in several review papers.[43−48] In our latest works, we described a method (called "seeding + growing") by which $Rh/TiO_2(110)-(1 \times 2)$ model catalyst surfaces with well-separated (50−100 nm) Rh nanoparticles with an average diameter of approximately 1−10 nm can be produced.[49,50] The method consists of two steps: (i) evaporation of 0.001−0.050 ML rhodium at room temperature with post-annealing at 1200 K ("seeding"); (ii) postdeposition of rhodium at 1200 K for further growing of the existing Rh nanocrystallites formed in the first step ("growing"). The main advantage of this method is the clear separation of the admetal nanoparticles, which makes possible an STM study of the nanoscale morphological changes in the region of an individual nanoparticle.

Figure 1a shows the clean $TiO_2(110)-(1 \times 2)$ surface on which Rh crystallites with a diameter of approximately 10 nm and a height of 4 nm were grown (Figure 1e). The total coverage of Rh is in the range of 1 ML. It can be seen that the particles exhibit mostly hexagonal shape but approximately 15% of them show elongated form. This behavior suggests the formation of two different types of crystallites: (111) or (100) face parallel to the support plane as described in detail in our earlier paper.[49]

Effect of CO on a Clean $TiO_2(110)-(1 \times 2)$ Surface. Figure 1a−d images depict the effect of treatment in 10 mbar CO at different temperatures for 10 min on the clean $TiO_2(110)-(1 \times 2)$ surface in order to compare the changes induced in the same experiments on a Rh-crystallite covered surface (presented below). Before CO treatments the clean surface shows 1×2 reconstructed terraces with a corrugation (vertical [Z] difference between the lowest and the highest point of an image) of approximately 1 nm on an area of 50 nm × 50 nm (Figure 1a). The rows running in the [001] crystallographic orientation are

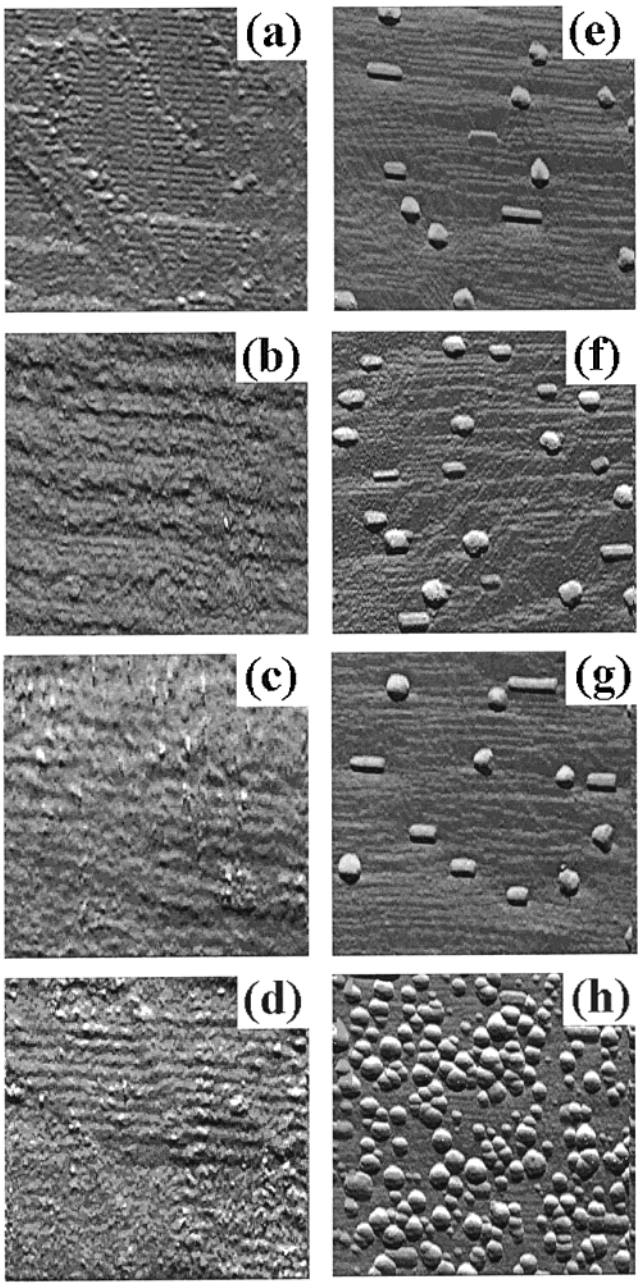

Figure 1. Effect of thermal treatment on the morphology of (a−d) clean and (e−h) Rh-covered $TiO_2(110)-(1 \times 2)$ surfaces in 10 mbar CO for 10 min (a, e) before the treatment and after annealing in CO at (b, f) 300 K, (c, g) 400 K, and (d, h) 500 K. Note the different scale of the STM images: (a−d) 50 nm × 50 nm; (e−h) 200 nm × 200 nm. Figure reduced to 66% for publication.

separated by 1.4 nm. This arrangement develops gradually into a well-ordered 1×4 structure clearly seen after CO exposure at 500 K (Figure 1b−d). The distance between the rows is 2.8 nm. Although some protrusions also appear, the $TiO_2(110)-(1 \times 4)$ surface is seemingly well ordered and flat. The original corrugation of the surface does not change perceptibly. It can be assumed that CO reacts with the surface and subsurface oxygen of TiO_2, resulting in its partial reduction. A small amount of surface carbon was detected after CO treatment, the intensity of the AES signal of C was about 0.15 that of Ti.

Formation of Carbon 3D Nanoclusters in the Presence of Rh Particles. In contrast with the clean $TiO_2(110)-(1 \times 2)$ surface, a totally different behavior was experienced for $Rh/TiO_2(110)-(1 \times 2)$ on the effect of the same treatments in CO. Figure 1e shows the model catalyst surface prepared by the

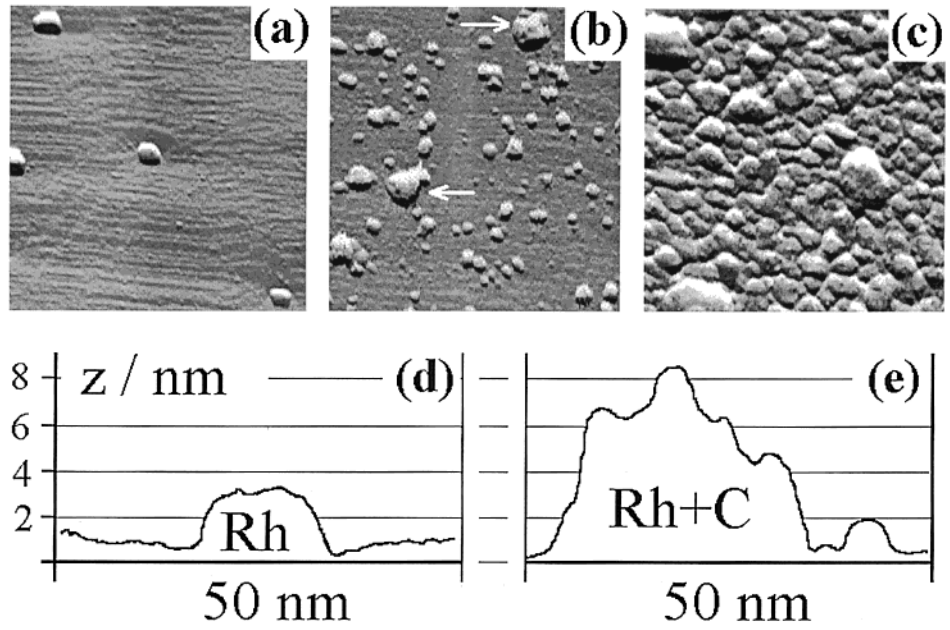

Figure 2. Effect of duration of the treatments of the $Rh/TiO_2(110)-(1 \times 2)$ surface in 10 mbar CO at 500 K: (a) before the treatment in CO and after treatment in CO for (b) 2 min and (c) 20 min. Line profiles through the center of an individual Rh particle (d) before CO treatment and (e) after 2 min CO treatment. The size of the STM images is 200 nm × 200 nm. Figure reduced to 66% for publication.

method described above (section "Preparation of Supported Rh Nanoparticles..."). Although no noticeable changes were recorded for exposures of CO at 300−400 K (Figure 1f,g), this surface exibits high activity in the formation of new 3D nanoparticles during the treatment in CO (10 mbar) at 500 K (Figure 1h). The apparent distribution of the extra round shape particles of 2−10 nm size is nonuniform; they form a grouplike structure on the surface. The most surprising feature is that new particles appear not only on the top of the originally present Rh nanoparticles but also on the free regions of the support. On the basis of STM images, it is difficult to distinguish between the original Rh clusters and the new particles; nevertheless, the existence of some elongated particles with nearly the same geometry as on the original $Rh/TiO_2(110)-(1 \times 2)$ surface suggests that the morphology of the Rh nanoparticles does not change; they are, however, partly covered by new nanoparticles. Moreover, the formation of new nanoparticles is accompanied by the appearance of the carbon signal in the AES. Whereas no C can be detected by AES on the cleaned Rh/TiO_2, the relative Auger-signal ratio for C(265 eV) and Ti(385 eV) was approximately 1 for the sample treated with CO at 500 K. This observation suggests that the newly appearing nanoparticles consist likely of carbon that develops on the admetal particles and diffuses as atomic carbon or a 1−2 nm nanocluster onto the support already at 500 K.

In the subsequent experiments the formation of carbon clusters was followed in time for supported Rh nanoparticles with an average diameter of 12−15 nm separated from each other by 60 nm on the average (Figure 2a). After exposure to CO (10 mbar) for 2 min at 500 K the STM images show larger particles of 20−25 nm in size (indicated by arrows) with nearly the same average separation as that of the original Rh nanoparticles and smaller new ones of 2−6 nm distributed on the surface region among the larger ones (Figure 2b). The region around an individual particle detected before and after CO treatment suggests a multiparticle covering layer on the top of the original metal crystallites, as it can be deduced from the line profiles running through the middle point of an original Rh particle and a carbon-covered one (Figure 2d,e). In the case represented by the STM image in Figure 2b the relative Auger-signal ratio for C(265 eV) and Ti(385 eV) is approximately 0.2. Further exposure to CO (10 mbar, 20 min, 500 K) results in total covering of the interparticle area of the support by particles of approximately 10 nm in size; nevertheless, the original ones with a larger diameter of 20−25 nm are still clearly distinguishable (Figure 2c). In this latter case AES shows practically only carbon. Two important remarks can be made: (i) both the average diameter and the height of the original Rh particles increases from 13 to 30 nm and from 2 to 8 nm, respectively; (ii) the size of carbon adclusters formed in the region between the Rh particles changes randomly (Figure 2b). These facts suggest that the formation of the extra 3D carbon nanoparticles of approximate diameter of 1−2 nm proceeds on the surface of Rh nanocrystallites with a subsequent migration to the free area of the support, resulting in the regeneration of active sites. If one supposes that only individual C atoms are mobile at 500 K, it would be expected that the size of the adparticles shows a radial decrease around the original Rh crystallites (source effect). But it is not the case: there are smaller and larger nanoparticles distributed randomly between the Rh crystallites. A Monte Carlo simulation study is in progress to receive deeper insight into this process.

Thermal Stability of the Carbon Nanoclusters Formed on the Rh/TiO_2 (110)−(1 × 2) Surface. Figure 3 shows the effect of consecutive annealing (10 min in each case) on the morphology of a carbon-covered surface (10 mbar CO, 500 K, 20 min) presented in Figure 2c. The annealing at 700 K results in a moderate change of the morphology, mainly in the collapse of the smaller particles (Figure 3a). This trend continues further on the effect of annealing at 800−1000 K without radical change of the corrugation in the 200 nm × 200 nm images (Figure 3b,c). The original corrugation of 14.5 nm (Figure 2c) increased up to 18.2 nm (Figure 3c), which means only an approximately 20% enhancement caused by the agglomeration and collapse of the particles. A tremendous increase in the corrugation (up to 31 nm) was experienced after annealing at 1100 and 1200 K: some of the particles became larger and the separation between them is more pronounced (Figure 3d,e). In this last

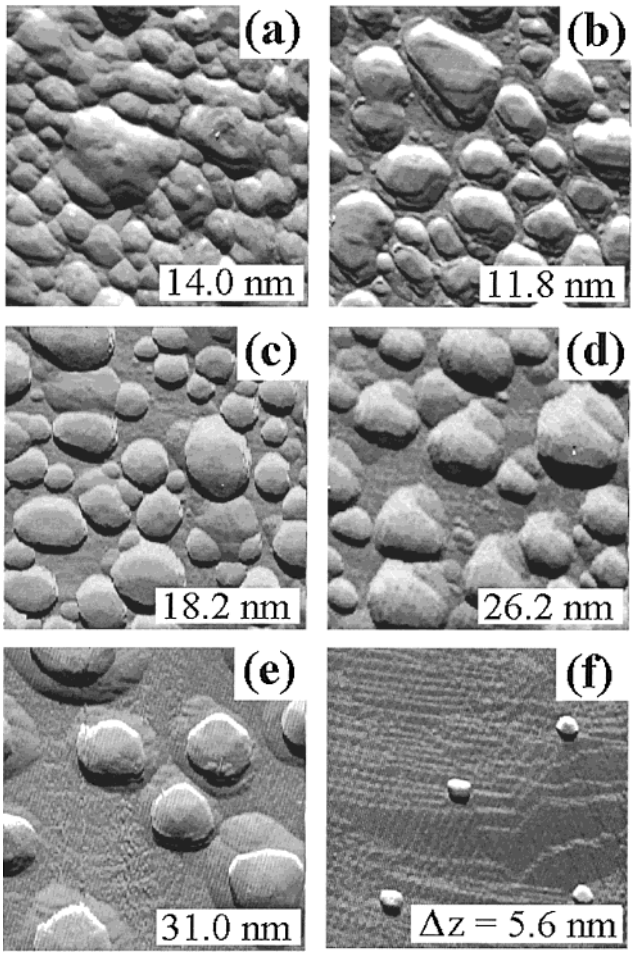

Figure 3. Effect of consecutive annealing (in UHV) at different temperatures of the CO-treated $Rh/TiO_2(110)-(1 \times 2)$ surface shown in Figure 2c (20 min, 10 mbar CO, 500 K): (a) 700 K; (b) 800 K; (c) 1000 K; (d) 1100 K; (e) 1200 K; (f) 1300 K. The corrugation (Δz) of the region is indicated at the right bottom of the images (200 nm × 200 nm). Figure reduced to 66% for publication.

stage the average diameter of the round shape particles is 40 nm, the height is approximately 25−30 nm (Figure 3e). The corrugation in the last case is 31 nm, which means 114% enhancement relative to that of the original structure shown in Figure 2a. The particles exhibit a surprisingly high aspect ratio of approximately 0.8. The average distance between them is nearly the same as that for the Rh nanoparticles on the original surface (compare Figure 3e and Figure 2a). We note that the stripe outlines perceptible around the particles are certainly the result of a tip convolution imaging artifact. The top face of these outrising hillocks is rather flat and parallel to the support surface. This fact suggests clearly that the carbon formed accumulates on and around the originally existing Rh crystallites, resulting in graphite "nanocakes". It is not clear yet whether Rh is dissolved uniformly in this structure or the compact Rh particles remained bonded to the titania support. More precise AES measurements and atomically resolved STM images are needed to decide this question and to characterize the surface of these curious nanostructures. Taking into account that the main mass of the outrising features on the images after annealing at 800 and 1200 K (Figure 3b,e, respectively) is carbon, we could calculate the decrease in the carbon content between 800 and 1200 K from the integrated particle volumes determined by STM. The calculation has shown that 80−90% of the surface carbon produced at 500 K in CO is stabilized in the "nanocake" form. The further annealing at 1300 K results in a recovering of the original morphology of the Rh particles distributed on the titania surface before CO treatment (Figure 3f). This can be clearly established by the comparison of this image with that in Figure 2a. The series of the STM images in Figure 3 suggests that on the effect of annealing the carbon nanoclusters accumulate on top of the Rh particles where the gasification of this carbon proceeds in the temperature range of 1200−1300 K, probably in an oxidation reaction by the bulk oxygen of the titania support. Analysis of gas evolved during linear heating (rate of 2 K/s) of the surface covered completely by carbon (as shown in Figure 2c) revealed that the main desorbing product is CO, which is released in the temperature range 800−1300 K. This observation is in good harmony with the structural changes detected by STM and supports the conclusion that the gasification of the deposited carbon proceeds by surface reaction with the segregated bulk oxygen of the support oxide.

Concluding Remarks

Adsorption of CO (10 mbar, 10 min) on a Rh-free TiO_2-$(110)-(1 \times 2)$ surface caused transformation of the (1×2) surface structure into the (1×4) arrangement at 500 K. The exposition of well-separated Rh nanoparticles (10−15 nm) deposited on $TiO_2(110)-(1 \times 2)$ to CO at 500 K produced a large amount of carbon clusters. The formation and migration of carbon species from the Rh particles onto the free area of the support can be readily followed by scanning tunneling microscopy. On the effect of heating in UHV the carbon clusters agglomerate and collapse into larger particles between 700 and 1100 K. The carbon deposits accumulate on the existing Rh nanoparticles at 1200 K. The recovering of the original $Rh/TiO_2(110)-(1 \times 2)$ morphology after annealing at 1300 K suggests a complete gasification (mainly into CO) of the carbon deposits by the bulk oxygen of the support.

Acknowledgment. This work was supported by the Hungarian Academy of Sciences and by grants of the Hungarian Scientific Research Fund (OTKA) T22869 and T29952.

References and Notes

(1) Somorjai, G. A. *Introduction to Surface Chemistry of Catalysis*; New York, 1994.
(2) Li, W.; Zhang, H.; Wang, C.; Zhang, Y.; Xu, L.; Zhu, K.; Xie, S. *Appl. Phys. Lett.* **1997**, *70*, 2684.
(3) Hernádi, K.; Fonesca, A.; Nagy, J. B.; Bernaerts, D.; Lucas, A. A. *Carbon* **1996**, *34*, 1249.
(4) Hernádi, K.; Fonesca, A.; Piedigrosso, P.; Delvaux, M.; Nagy, J. B.; Bernaerts, D.; Riga, J. *Catal. Lett.* **1997**, *48*, 229.
(5) Yudasaka, M.; Kikuchi, R.; Ohki, Y.; Ota E.; Yoshimura, S. *Appl. Phys. Lett.* **1997**, *70*, 1817.
(6) Dai, H.; Rinzler, A. G.; Nikolaev, P.; Thess, A.; Colbert, D. T.; Smalley, R. E. *Chem. Phys. Lett.* **1996**, *260*, 471.
(7) Chen, P.; Zhang, H. B.; Liu, G. D.; Hong, Q.; Tsai, K. R. *Carbon* **1997**, *35*, 1495.
(8) Khassin, A. A.; Yuirera, T. M.; Zaikovskij, V. J.; Parmon, V. N. *React. Kinet. Catal. Lett.* **1998**, *64*, 63.
(9) Kong, J.; Cassel, A. M.; Dai, H. *Chem. Phys. Lett.* **1998**, *292*, 567.
(10) Satishkumar, B. C.; Govindaraj, A.; Sen, R.; Rao, C. N. R. *Chem. Phys. Lett.* **1998**, *293*, 47.
(11) Maiti, A.; Brabec, C. J.; Bernhole, J. *Phys. Rev. B* **1997**, *55*, R6097.
(12) Yudasaka, M.; Kikuchi, R.; Matsui, T.; Ohki, Y.; Yoshimura, S.; Ohta, E. *Appl. Phys. Lett.* **1995**, *67*, 2477.
(13) Cheng, H. M.; Li, F.; Sun, X.; Brown, S. D. M.; Pimenta, M. A.; Marucci, A.; Dresselhaus, G.; Dresselhaus, M. S. *Chem. Phys. Lett.* **1998**, *289*, 602.
(14) Terrones, M.; Grobert, N.; Zhang, J. P.; Terrones, H.; Olivares, J.; Hsu, W. K.; Hare, J. P.; Cheetham, A. K.; Kroto, H. W.; Walton, D. R. M. *Chem. Phys. Lett.* **1998**, *285*, 299.
(15) Fonesca, A.; Hernadi, K.; Nagy, J. B.; Lambin, Ph.; Lucas, A. A. *Carbon* **1995**, *33*, 1759.
(16) van't Blik, H. F. J.; van Zon, J. B. A. D.; Huizinga, T.; Vis, J. C.; Koningsberger, D. C.; Prins, R. *J. Am. Chem. Soc.* **1985**, *107*, 3139.

(17) Solymosi, F.; Pásztor, M. *J. Phys. Chem.* **1995**, *89*, 4783.
(18) Solymosi, F.; Bánsági, T. *J. Phys. Chem.* **1993**, *97*, 10133 and references therein.
(19) Solymosi, F.; Raskó, J. *J. Catal.* **1989**, *115*, 107.
(20) Mizushims, T. M.; Thoji, K.; Udagawa, Y. *J. Phys. Chem.* **1990**, *94*, 4980.
(21) Solymosi, F.; Novák, É.; Molnár, Á. *J. Phys. Chem.* **1990**, *94*, 7250.
(22) Solymosi, F.; Bánsági, T. *J. Phys. Chem.* **1992**, *96*, 11349.
(23) Guczi, L.; Beck, A.; Zsoldos, Z.; Dobos, S. *J. Mol. Catal.* **1989**, *56*, 50.
(24) Berkó, A.; Ménesi, G.; Solymosi, F. *J. Phys. Chem.* **1996**, *100*, 17732.
(25) Berkó, A.; Solymosi, A. *Surf. Sci.* **1998**, *411*, L900.
(26) Berkó, A.; Solymosi, F. *J. Catal.* **1999**, *183*, 91.
(27) Bäumer, M.; Frank, M.; Libuda, J.; Stempel, S.; Freund, H.-J. *Surf. Sci.* **1997**, *391*, 204.
(28) Solymosi, F.; Erdöhelyi, A. *Surf. Sci.* **1981**, *110*, L630.
(29) Erdöhelyi, A.; Solymosi, F. *J. Catal.* **1983**, *84*, 446.
(30) Marbrow, R. A.; Lambert, R. M. *Surf. Sci.* **1977**, *67*, 489.
(31) Castner, D. G.; Sexton, B. A.; Somorjai, G. A. *Surf. Sci.* **1978**, *71*, 519.
(32) Castner, D. G.; Somorjai, G. A. *Surf. Sci.* **1979**, *83*, 60.
(33) Dubois, L. H.; Somorjai, G. A. *Surf. Sci.* **1980**, *91*, 514.
(34) Yates Jr. J. T.; Williams, E. D.; Weinberg, W. H. *Surf. Sci.* **1980**, *91*, 562.
(35) Castner, D. G.; Dubois, L. H.; Sexton, B. A.; Somorjai, G. A. *Surf. Sci.* **1981**, *103*, L134.
(36) DeLouise, L. A.; Winograd, N. *Surf. Sci.* **1984**, *138*, 417.
(37) Rebholz, M.; Prins, R.; Kruse, N. *Surf. Sci.* **1991**, *259*, L797.
(38) Rebholz, M.; Prins, R.; Kruse, N. *Surf. Sci.* **1992**, *269/270*, 293.
(39) Frank, M.; S: Andersson, S.; Libuda, J.; Stempel, S.; Sandell, A.; Brena, B.; Giertz, A.; Brühwiler, P. A.; Bäumer, M.; Mårtensson, N.; Freund, H.-J. *Chem. Phys. Lett.* **1997**, *279*, 92.
(40) Andersson, S.; Frank, M.; Sandell, A.; Giertz, A.; Brena, B.; Brühwiler, P. A.; Mårtensson, N.; Libuda, J.; Bäumer, M.; Freund, H.-J. *J. Chem. Phys.* **1998**, *108*, 2967.
(41) Berkó, A.; Ménesi, G.; Solymosi, F. *Surf. Sci.* **1997**, *372*, 202.
(42) Berkó, A.; Solymosi, F. *Langmuir* **1996**, *12*, 1257.
(43) Campbell, C. T. *Surf. Sci. Rep.* **1997**, *27*, 1.
(44) Henry, C. R. *Surf. Sci. Rep.* **1998**, *31*, 231.
(45) Günter, P. L. J.; Niemantsverdriet, J. W.; Riberio, F. H.; Somorjai, G. A. *Catal. Rev.* **1997**, *39*, 77.
(46) Diebold, U.; Pan, J. M.; Madey, T. E. *Surf. Sci.* **1995**, *331*−*333*, 845.
(47) Goodman, D. W. *Surf. Rev. Lett.* **1996**, *2*, 9.
(48) Lad, R. J. *Surf. Sci. Lett.* **1995**, *2*, 109.
(49) Berkó, A.; Solymosi, F. *Surf. Sci.* **1998**, *400*, 281.
(50) Berkó, A.; Klivényi, G.; Solymosi, F. *J. Catal.* **1999**, *182*, 511.